Optical effects of annealing on Yb-doped Y_2SiO_5 thin films

2007 J. Phys.: Condens. Matter 19 156222

(http://iopscience.iop.org/0953-8984/19/15/156222)

IOP PUBLISHING JOURNAL OF PHYSICS: CONDENSED MATTER

J. Phys.: Condens. Matter **19** (2007) 156222 (8pp) doi:10.1088/0953-8984/19/15/156222

Optical effects of annealing on Yb-doped Y_2SiO_5 thin films

A Denoyer[1], S Jandl[1], F Thibault[2] and D Pelenc[2]

[1] Département de Physique de l'Université de Sherbrooke, Sherbrooke, QC, J1K 2R1, Canada
[2] CEA-Grenoble LETI/DOPT/STCO, 17 rue des Martyrs, 38054 Grenoble cedex 09, France

E-mail: aurelie.denoyer@usherbrooke.ca

Received 8 December 2006, in final form 6 March 2007
Published 26 March 2007
Online at stacks.iop.org/JPhysCM/19/156222

Abstract

In this paper we investigate the optical effects of annealing under an oxygen atmosphere of Yb-doped Y_2SiO_5 thin films grown by liquid phase epitaxy. Infrared transmission, particularly adapted to thin film characterizations by means of Yb^{3+} crystal field excitations, is used to single out the effects of annealing. For instance, absorption intensities increase by $\sim$10% and disorder in Yb^{3+} substitution is reduced. Micro-Raman backscattering measurements detect no particular defects in as-grown and annealed thin films.

1. Introduction

Rare earth solid state lasers emitting around 1 μm are of current interest for several applications such as frequency doubling, optical bistability, amplifiers, power lasers and telecommunication. Recently, Yb^{3+}-based laser materials appeared as possible competitors to replace Nd^{3+}-based solid lasers (Nd^{3+}:YAG). These materials present numerous advantages resulting from a simple electronic structure, with just two manifold levels ($^2F_{7/2}$ and $^2F_{5/2}$), which prevents self-quenching by cross-relaxation and up-conversion parasitic effects [1]. They have large absorption bands, needed for diode pump temperature drift compensation or laser tuning and above all for ultra-short laser pulses. Hence, realization of femtosecond oscillators [2–5] and amplifiers [6] are made possible thanks to their broad emission bands. Orthosilicates, which are already used intensively in photonic applications [7–9], have demonstrated efficient laser action [10, 11] because of their large fundamental manifold splitting (allowing a quasi-three level laser configuration). In particular, Yb-doped Y_2SiO_5 (Yb:YSO) has one of the largest crystal-field splittings [12] and exhibits more than 7 W laser power radiation around 1 μm under 14.4 W diode pumping at 978 nm, leading to high optical conversions of around 50%. It also shows little sensitivity to pump wavelength drift and presents broad tunability (more than 4 W of emitted power over 60 nm) [13] and has good thermal properties (thermal conductivity of 4.4 W m^{-1} K^{-1}), which is an important feature for lasers [14].

This paper follows up the study of Yb-doped Y_2SiO_5 thin films grown by liquid phase epitaxy (LPE) [15–17]. Such films are good candidates for waveguide lasers for integrated

Table 1. Mass changes before and after annealing for different samples of Yb14%:YSO.

Annealing	3 h, 1000 °C	3 h, 1200 °C	12 h, 1200 °C
Mass change after annealing (%)	−0.06 [a]	+0.02	+0.33

[a] Release of incorporated Pb ions, see text.

optics. They can be strongly doped (up to ∼20%) allowing miniaturization without introducing significant disorder and inhomogeneities. In this study we investigate the optical properties of annealed Yb:YSO thin films under an oxygen atmosphere. Actually, impurities of divalent rare earth ions have often been reported in different crystals, and especially Yb^{2+} due to its favourable complete 4f shell [18–20]. Annealing under an oxygen atmosphere after LPE converts Yb^{2+} impurities into Yb^{3+}. Preliminary measurements of propagation loss indicate that losses are reduced by up to ∼100% for 24% Yb-doped thin films and the refractive index is reduced (which is interesting for monomode guide elaboration); both features attributable to possible elimination of Yb^{2+} ion impurities. Infrared transmission, particularly adapted to thin film characterization, is used to single out the effects of impurities and the effects of annealing on Yb:YSO thin films. In particular Yb^{3+} crystal field excitation intensities and bandwidths as well as Yb^{3+}–Yb^{3+} pair satellites (as observed and described in [15, 21–25]) are analysed. Besides, a Raman active phonon study confirms the absence of important defects in either as-grown or annealed thin films.

2. Experimental setting

Y_2SiO_5 (YSO) crystallizes in the C^6_{2h} monoclinic space group [26]. Yb^{3+} ions substitute equally the two non-equivalent C_1 symmetry Y^{3+} sites of the host lattice, with coordination number (6 + 1) for Y_I (mean Y–O distance 2.309 Å) and 6 for Y_{II} (mean Y–O distance 2.269 Å). Y^{3+} and Yb^{3+} have similar ionic radii (0.96 and 0.92 Å, respectively), so that no noticeable defects or strains are introduced. The studied thin films were all produced from the same original sample: a 1.7 μm-thick Yb14%:Y_2SiO_5 thin film grown by liquid phase epitaxy (LPE). LPE was realized on undoped YSO substrate with (010)-orientation from a Czochralski grown crystal. The epitaxial melt consisted of a mixture of silica and rare earth oxides into a PbO–B_2O solvent, and growth temperatures were in the 950–1050 °C range. In appropriate experimental conditions, the introduction of a single crystal substrate (used as the seed) into the supersaturated melt induces the growth of a single crystal layer on the two substrate faces [27]. Due to segregation, the Yb thin film concentration turned out to be 20% larger than in the epitaxial melt. The sample was then cut into several pieces: one piece was kept as a reference while the others were annealed under an air + O_2 atmosphere at ambient pressure for 3–12 h, and at temperatures varying from 1000 to 1200 °C. Mass increases were measured (up to +0.33% after annealing), indicating that oxygen was incorporated in the annealing process (see table 1).

In some cases the mass of the thin film could decrease due to the release of Pb ions incorporated during the growth process [28]. In the case of incomplete migration, such ions segregate to form Pb oxide on the thin film surface and affect the infrared transmission baseline. Dipping the thin film in a nitric acid/acetic acid/water (1/3, 1/3, 1/3) solution at 60 °C for 20 min, dissolves the deposit and restores the infrared baseline.

For the infrared measurements, the samples were mounted on a closed-cycle cryostat cold finger. 0.5 cm^{-1} resolution transmission spectra at $T = 13$ K were obtained with incident light

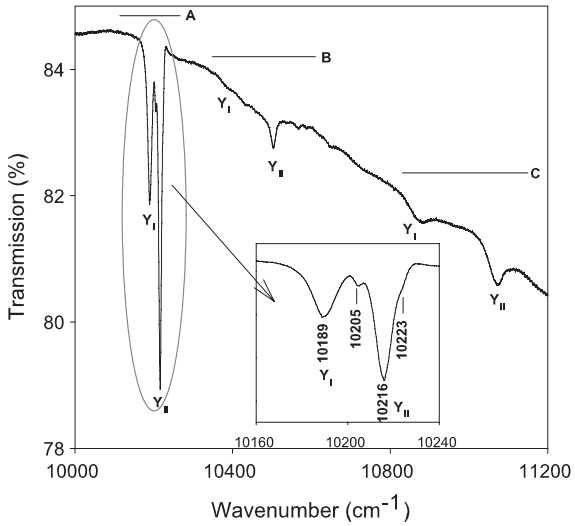

Figure 1. Infrared spectrum at $T = 13$ K of the reference Yb14%:YSO thin film. Regions A, B and C stand for $^2F_{7/2}(0) \rightarrow {}^2F_{5/2}(0)$, $^2F_{7/2}(0) \rightarrow {}^2F_{5/2}(1)$ and $^2F_{7/2}(0) \rightarrow {}^2F_{5/2}(2)$ transmissions, respectively. Inset: $^2F_{7/2}(0) \rightarrow {}^2F_{5/2}(0)$ expanded range.

perpendicular to the (010) crystal plane, in the 9000–15 000 cm^{-1} energy range, using a Fourier transform interferometer (BOMEM DA3.002) equipped with a quartz-halogen source, a quartz beamsplitter and a Si detector.

Micro-Raman backscattering spectra were recorded at room temperature using a Labram 800 spectrometer equipped with a 50× objective, an appropriate notch filter and a nitrogen cooled charge-coupled-device (CCD) detector. A polarized 632.8 nm He–Ne laser line, focused to ∼3 μm spot diameter, was used for excitation.

3. Infrared absorption results

The energy levels of the Yb^{3+} ions split in two main manifolds: $^2F_{7/2}$ (four degenerate Kramers doublets) and $^2F_{5/2}$ (three degenerate Kramers doublets) once embedded into a host crystal. Due to the low site symmetries, the three expected absorption bands, ($^2F_{7/2}(0) \rightarrow {}^2F_{5/2}(0)$, $^2F_{7/2}(0) \rightarrow {}^2F_{5/2}(1)$ and $^2F_{7/2}(0) \rightarrow {}^2F_{5/2}(2)$), are observed for each site (figure 1). This study particularly focuses on the $^2F_{7/2}(0) \rightarrow {}^2F_{5/2}(0)$ ((A) in figure 1) region due to its narrow and intense absorption bands, as compared to absorption bands (B) and (C) which are broad and affected by vibronics superposition. Previous works have been carried out on Yb:YSO thin films and single crystals [21, 15, 17] pointing out the presence of magnetically coupled Yb^{3+}–Yb^{3+} pairs, as described by Guillot-Noël *et al* [22, 29]. Ferromagnetic and antiferromagnetic exchange interactions are observed; notably the bands located at 10 205 cm^{-1} and at 10 223 cm^{-1} are associated with ferromagnetic and antiferromagnetic interactions, respectively [21, 15]. They correspond to Yb^{3+}–Yb^{3+} ion pairs, with both Yb^{3+} ions located in Y_{II} sites.

3.1. Absorption intensity

Infrared transmission spectra have been fitted with mixed Gaussian–Lorentzian bands, allowing the thin film absorption intensities (spectrum area), which are proportional to Yb^{3+}

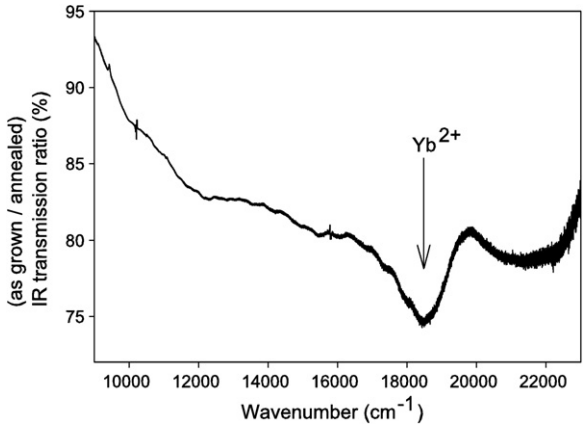

Figure 2. (As-grown/annealed) thin film infrared transmission ratio. The pronounced absorption band around 18 000 cm^{-1} could be associated with the Yb^{2+} energy level in the as-grown thin film.

Table 2. Absorption intensity increases for different annealed samples of Yb14%:YSO.

Sample	Reference	3 h, 1000 °C	3 h, 1200 °C	12 h, 1200 °C
Absorption intensity increase	0%	2%	10%	10%

concentration, to be measured. In Yb-doped YAG crystals, Yb^{2+} ions associated with colour centres and lattice distortions have been identified [30]. We conjecture that Yb^{2+} impurities are present in Yb:YSO similarly to Yb:YAG. Actually, during the growth process Y_2SiO_5 oxygen vacancies generate colour centres that can accommodate Yb^{2+}. In the annealing process, oxygen vacancies are eliminated and Yb^{2+} are converted to Yb^{3+}. In figure 2, the thin film infrared transmission ratio (as-grown/annealed) shows a pronounced absorption band around 18 000 cm^{-1} that could be associated, in the as-grown thin films, with the Yb^{2+} energy level [30]. This absorption band disappears after annealing, indicating the conversion of Yb^{2+} in Yb^{3+}. Due to the release of Pb ions incorporated during thin film growth during the annealing process, it is difficult to establish a clear correlation between the mass increase of table 1 and the absorption increase of table 2. As expected, the absorption is larger with annealing (up to ∼10% larger) which indicates the effective oxidation of Yb^{2+} ions into Yb^{3+} (figure 3 and table 2). Besides, for higher annealing temperatures greater absorptions are observed (absorption intensity at 1000 °C (3 h) is 93% ± 2 of the absorption intensity at 1200 °C (3 h)). However, there is no noticeable difference in absorption intensities between 3 and 12 h annealing at 1200 °C. Thus, after 3 h annealing at 1200 °C, we can assume that all Yb^{2+} impurities have been oxidized.

3.2. Yb^{3+} ion sites rearrangement

The evolution of the relative intensity of the bands, reflecting relative site populations, is shown in figure 3, indicating a reorganization of Yb^{3+} in the host crystal. In fact, for a short annealing time (3 h) there is no real change in the relative intensities of the bands; each band grows almost identically, meaning that eventual Yb^{2+} ions were probably distributed randomly in all

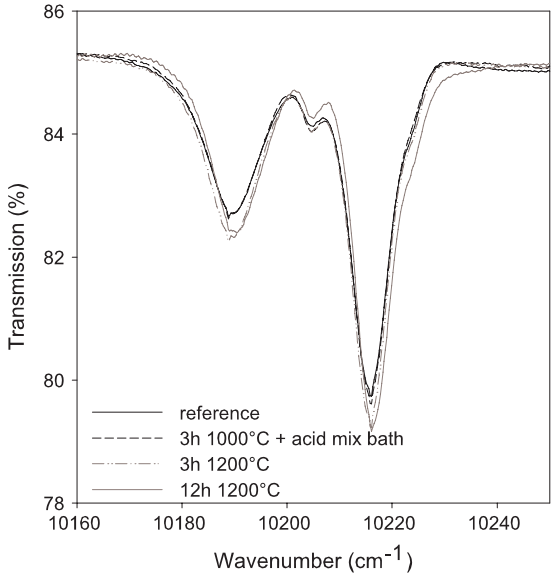

Figure 3. Infrared spectra at $T = 13$ K showing the absorption intensity differences for Yb14%:YSO as-grown and annealed thin films.

Table 3. Y_I population (%) for different annealed samples of Yb14%:YSO.

Sample	Reference	3 h, 1000 °C	3 h, 1200 °C	12 h, 1200 °C
$Y_I/(Y_I + Y_{II})$ (%)	45 ± 1	43 ± 2	43 ± 2	36 ± 2

possible sites. For a longer annealing time (12 h), the total population of Y_{II} increases, so that it can be asserted that Y_{II} is thermodynamically more stable than Y_I in the thin films, which confirms previous conclusions [15, 17]. Actually, Y_I varies from ∼45% ± 1 to ∼36% ± 2 for 12 h annealing at 1200 °C (see table 3); this ratio change is partly due to the growth of the Y_{II} satellite band.

As shown in figures 3 and 4, satellites due to Yb^{3+}–Yb^{3+} pairs evolve following annealing. Notably, the area of the satellite attributed to antiferromagnetic interactions (10 223 cm^{-1} band) grows from ∼6 to 16% of the total Y_{II} population with annealing time. This is to the detriment of ferromagnetic pairs (10 205 cm^{-1} band) which vary from ∼8 to 5% of the total Y_{II} population. We can assume that antiferromagnetic pairs are favoured thermodynamically and the tendency is reversed compared to the reference as shown in figure 4. Total pair contributions are also enhanced (from 8 to 13% of the total $Y_I + Y_{II}$ population).

Thus, once oxidation is completed, Yb^{3+} ions rearrange in more stable states, increasing ordering as confirmed by narrower bandwidths. For instance, the Y_I regular site bandwidth (located at 10 189 cm^{-1}) is reduced from 12.8 to 11.8 cm^{-1} (−7.5%) for 12 h annealing at 1200 °C. The same reduction is observed for the Y_{II} regular site bandwidth (located at 10 216 cm^{-1}).

The crystal field excitation frequencies also shift slightly, as can be seen in figure 3. For instance two very close bands seem to be in competition for the Y_I regular site $^2F_{7/2}(0) \rightarrow {}^2F_{5/2}(0)$ transition, and annealing favours one of these two bands: 10 188.8 → 10 190.5 cm^{-1}. A bulge, associated with Yb^{3+}–Yb^{3+} pairs, also appears toward higher energies

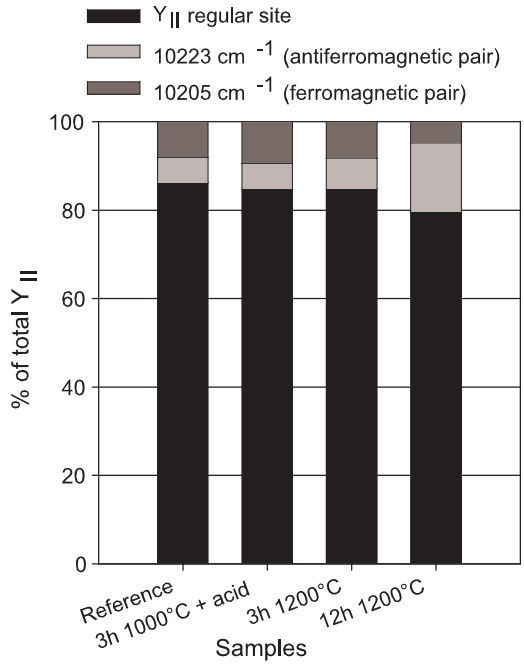

Figure 4. Y_{II} distribution between isolated Yb^{3+} ions (regular site) and Yb^{3+}–Yb^{3+} pairs either ferromagnetic (10 205 cm^{-1}) or antiferromagnetic (10 223 cm^{-1}) of different Yb14%:YSO annealed thin films.

for the Y_{II} regular site transition with long-time annealing. This indicates that bands attributed to pair interactions are better resolved due to narrower bandwidths following annealing.

4. Raman scattering results

A detailed analysis of Yb:YSO single crystal phonons has been previously carried out [21]. Due to the low point group symmetry of the crystal, C_{2h}^6, a large number of phonons are expected, and $48A_g$ and $48B_g$ modes are actually Raman active. Raman spectra are of interest for detecting defects as well as local modes. Yb doping results in a broadening and redshift of the low frequency phonons (<350 cm^{-1}), as expected from the Y^{3+} and the Yb^{3+} mass differences, while the high frequency Si–O vibrations remain unaffected [21]. For comparison purposes, Yb15%:YSO single crystal and thin film spectra are given in figure 5 showing that thin film Raman active phonons are identical to the single crystal in terms of A_g and B_g frequencies. The three main phonon groups dominated by Y (<350 cm^{-1}); Y–O, Si–O (500–700 cm^{-1}); and O (>800 cm^{-1}) vibrations are observed in as-grown annealed thin films and Yb:YSO single crystal.

Phonon bandwidths, that are inversely proportional to lifetimes which depend on defects and strains, are probed successfully with micro-Raman spectroscopy to show possible annealing effects on A_g and B_g Raman active phonons. No significant differences are observed between the reference thin film and the thin films annealed in different conditions (figure 5). Actually, phonon frequencies and bandwidths remain almost the same at approximately ± 0.1 cm^{-1}. The overall narrower phonon bandwidths in the thin films as compared to the doped single crystal and as reported in table 2 of [17] attest to their high quality even before annealing.

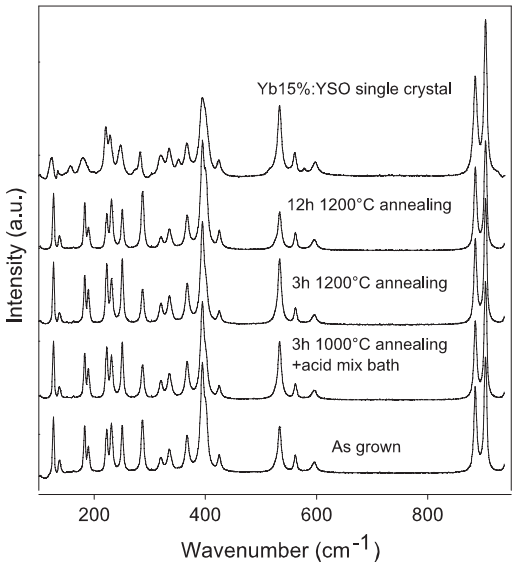

Figure 5. Micro-Raman spectra at room temperature of Yb14%:YSO as-grown and annealed thin films and Yb15%:YSO single crystal.

Besides, the absence of additional or local modes confirms that neither surface defects nor contamination are produced during the growing and annealing processes. Still Raman scattering is not sensitive enough to track Yb^{2+} or to show subtle differences like Yb^{3+} site relative occupations.

5. Conclusion

Crystal field excitations appear to be particularly sensitive and suitable for the study of small changes induced by annealing processes in doped thin films, contrary to micro-Raman scattering which is not sensitive enough to probe minor differences. From an optical point of view, Yb:YSO thin film annealing processes have relatively small but interesting effects, like confirming oxidation of Yb^{2+} and removal of PbO introduced during LPE. Also this study underlines the different steps in defect free annealing: first removal of PbO and possible oxidation of Yb^{2+} followed by ordering of Yb^{3+} ions in the lattice into their most stable states (Y_{II} and selective pair formation). The optical and lasing properties of thin films are improved following annealing. Also, annealing could be used to enhance or optimize characteristics required for some applications like laser tunability and ultra-short laser pulse generation.

Acknowledgments

We thank J Rousseau and M Castonguay for technical assistance. A Denoyer and S Jandl acknowledge support from the National Science and Engineering Research Council of Canada and the Fonds Québécois de la Recherche sur la Nature et les Technologies.

References

[1] Sumida D S and Fan T Y 1995 *Opt. Lett.* **20** 2384
[2] Thibault F, Pelenc D, Druon F, Zaouter Y, Jacquemet M and Georges P 2006 *Opt. Lett.* **31** 1555

[3] Brunner F, Spühler G J, Aus der Au J, Krainer L, Morier-Genoud F, Paschotta R, Lichtenstein N, Weiss S, Harder C, Lagatsky A A, Abdolvand A, Kuleshov N V and Keller U 2000 *Opt. Lett.* **25** 1119
[4] Druon F, Chénais S, Raybaut P, Balembois F, Georges P, Gaumé R, Haumesser P H, Viana B, Vivien D, Dhellemmes S, Ortiz V and Larat C 2002 *Opt. Lett.* **27** 1914
[5] Druon F, Chénais S, Raybaut P, Balembois F, Georges P, Gaumé R, Aka G, Viana B, Mohr S and Kopf D 2002 *Opt. Lett.* **27** 197
[6] Raybaut P, Druon F, Balembois F, Georges P, Gaumé R, Viana B and Vivien D 2003 *Opt. Lett.* **28** 2195
[7] Van Eijk Carel W E 1997 *Nucl. Instrum. Methods Phys. Res.* A **392** 285
[8] Comaskey B, Albrecht G F, Velsko S P and Moran B D 1994 *Appl. Opt.* **33** 6377
[9] Chang C K, Chang J Y and Kuo Y K 2002 *Proc. SPIE High Power Lasers and Applications* vol 4914 (Bellingham, WA: SPIE) pp 498–509
[10] Li C, Moncorgé R, Souriau J C, Borel C and Wyon C 1994 *Opt. Commun.* **107** 61
[11] Gaumé R, Haumesser P H, Viana B, Aka G, Vivien D, Scheer E, Bourdon P, Ferrand B, Jacquet M and Lenain N 2000 *Adv. Solid-State Laser* **34** 469
[12] Haumesser P H, Gaumé R, Viana B, Antic-Fidancev E and Vivien D 2001 *J. Phys.: Condens. Matter* **13** 5427
[13] Jacquemet M, Jacquemet C, Janel N, Druon F, Balembois F, Georges P, Petit J, Viana B, Vivien D and Ferrand B 2005 *Appl. Phys.* B **80** 171
[14] Gaumé R, Viana B, Derouet J and Vivien D 2003 *Opt. Mater.* **22** 107
[15] Denoyer A, Jandl S, Viana B, Guillot-Noël O, Goldner P, Pelenc D and Thibault F 2006 *Proc. SPIE* **6190** 287
[16] Thibault F, Pelenc D, Couchaud M, Chambaz B, Ferrand B, Druon F, Zaouter Y, Jacquemet M and Georges P 2005 Laser de forte puissance et production d' impulsions femtosecondes dans des cristaux d' YSO et LSO dopés ytterbium—Croissance de couches minces pour application laser *JNCO2005,* 14/12/2005
[17] Denoyer A, Jandl S, Viana B, Guillot-Noël O, Goldner P, Pelenc D and Thibault F 2007 Optical properties of Yb-doped Y_2SiO_5 thin films *Opt. Mater.* at press
[18] Kaczmarek S M, Tsuboi T, Ito M, Boulon G and Leniec G 2005 *J. Phys.: Condens. Matter* **17** 3771
[19] Voyer C J, Ryan D H, Ahn K, Gschneider K A Jr and Pecharsky V K 2006 *Phys. Rev.* B **73** 174422
[20] Wojtowicz A J, Lempicki A, Wisniewski D, Balcerzyk M and Brecher C 1994 *Nuclear Science Symp. and Medical Imaging Conf., 1994 IEEE Conf. Record*
[21] Campos S, Denoyer A, Jandl S, Vivien D, Loiseau P and Ferrand B 2004 *J. Phys.: Condens. Matter* **16** 4579
[22] Guillot-Noël O, Metha V, Viana B, Gourier D, Boukhris M and Jandl S 2000 *Phys. Rev.* B **61** 15338
[23] Jandl S, Guillot-Noël O and Gourier D 2002 *Opt. Mater.* **19** 449
[24] Boukhris M, Jandl S, Guillot-Noël O, Gourier D and Gesland J Y 2002 *J. Phys. Chem. Solids* **63** 525
[25] Mehta V, Guillot-Noël O, Gourier D, Ichalalène Z, Castonguay M and Jandl S 2000 *J. Phys.: Condens. Matter* **12** 7149
[26] Maksimov B A, Ilyukhin V V, Kharitonov U A and Belov N V 1970 *Kristallografiya* **15** 926
[27] Ferrand B, Chambaz B and Couchaud M 1999 *Opt. Mater.* **11** 101
[28] Priggemeyer S, Koschmieder H, Van Wyk G N and Heiland W 1991 *Fresenius J. Anal. Chem.* **341** 343
[29] Guillot-Noël O, Goldner P, Higel P and Gourier D 2004 *J. Phys.: Condens. Matter* **16** R1–24
[30] Yang P, Deng P and Yin Z 2002 *J. Lumin.* **97** 51